Polymorphism in Syndiotactic Polypropylene: Thermodynamic Stable Regions for Form I and Form II in Pressure−Temperature Phase Diagram

S. Rastogi,*,† D. La Camera,† F. van der Burgt,† A. E. Terry,‡ and S. Z. D. Cheng§

The Dutch Polymer Institute, Eindhoven Polymer Laboratories, P.O. Box 513, 5600MB Eindhoven, The Netherlands; European Synchrotron Radiation Facility, BP220, F-38043 Grenoble, France; and Department of Polymer Science, University of Akron, Akron, Ohio 44325-3909

Received May 25, 2001; Revised Manuscript Received July 29, 2001

ABSTRACT: Polymorphism is a general phenomenon observed in polymers. Syndiotactic polypropylene also exhibits polymorphism, and four limited-ordered modifications have been proposed so far. These modifications are commonly known as form I, II, III, and IV. Form I is normally obtained on cooling an isotropic melt at atmospheric pressure. By in-situ X-ray studies performed at elevated pressure−temperature, we show that, for the first time, form II can be also obtained on cooling the isotropic melt at high pressures. When investigated by NMR, the form II thus obtained is found to be free from conformational defects. We observed that above 1.5 kbar the melting temperature of form II is higher than that of form I. This is in contradiction to the melting behavior of the two different forms below 1.5 kbar; that is, the melting temperature of form II (crystallized at pressures greater than 1.5 kbar) is found to be always lower than for form I below 1.5 kbar. On cooling from the isotropic melt, below 1.5 kbar, the sample crystallizes in the ordered form I. These findings suggest presence of a thermodynamically stable region for form II in the pressure−temperature phase diagram. The difference in crystallization kinetics of the two phases has been also followed at different pressures.

1. Introduction

Syndiotactic polypropylene is a semicrystalline polymer presenting a complex polymorphism.[1−11] Four limited-ordered crystal forms have been described so far. Following the standard nomenclature, form I and II contain polymer chains in **s**(2/1)2 helical conformation $(TTGG)_n$ and form III is characterized by s-PP chains in the trans-planar conformation $(TT)_n$ whereas in form IV chains adopt a $(T_6G_2T_2G_2)_n$ conformation. Besides these four limited-ordered structures, the polymorphic forms of s-PP present different kinds and degrees of disorder depending upon the mechanical and thermal history of crystallization and degree of stereoregularity of the polymer.[12−16]

Form I is considered to be the thermodynamically stable phase for s-PP obtained on cooling from the melt and/or precipitation from solution at atmospheric pressure.[4,7,17] The proposed model for the limited-ordered crystal structure of form I, as first described by Lotz and Lovinger,[4,7] is characterized by an antichiral packing of the **s**(2/1)2 helical chains of s-PP, along both the *a* and *b* axes of an orthorhombic unit cell, with $a = 1.45$ nm, $b = 1.12$ nm, and $c = 0.74$ nm, according to the space group *Ibca*. The limited-ordered crystal structure of form I was later refined by De Rosa, Auriemma, and Corradini.[18] By slight modification of the crystal structure proposed by Lotz-Lovinger, De Rosa et al. suggested a model, characterized by s-PP chains packed according to the symmetry of the space group $P2_1/a$. A slightly different unit cell with dimensions $a = 1.43$ nm, $b = 1.11$ nm, $c = 0.75$ nm, and $\gamma = 90.3°$ was proposed. However, in this model, like for the space group *Ibca*, the antichiral packing of the **s**(2/1)2 helical chains of s-PP, along both the *a* and *b* axes, is maintained and also the position of the chain axis remains unchanged.

Different kinds and degrees of disorder have been described for form I.[4−7] In this paper, the term "form I perfect" (I_{per}) will be used for the limited-ordered form I of s-PP. The diagnostic reflections for form I_{per} are the appearance of reflections at 4.4 and 4.7 Å. The intensity and presence of these two reflections changes with crystallization conditions. As mentioned above, this form is characterized by an antichiral packing both in the *a* and *b* axes of the unit cell. Crystallization in form I_{per} occurs when the polymers, with high stereoregularity, are left to anneal close to the equilibrium melting point.[6,7,18]

The form I normally obtained from the melt, without presence of the reflection at 4.4 Å will be assigned as form I_{imp}. The disordered form I has been obtained in samples that were crystallized in rapidly precipitated powders from solution or during isothermal crystallization at low temperature, in samples having a different degree of syndiotacticity.[4,7,8,15,17] Again, the experimental observations show that the kind and degree of disorder strongly depends on the crystallization history and stereoregularity of the polymer.[4,7,17]

Form II of s-PP as described by Corradini and Natta et al.[2] is characterized by **s**(2/1)2 helices of the same chirality, packed according to the space group $C222_1$, in an orthorhombic unit cell, $a = 1.45$ nm, $b = 0.56$ nm, and $c = 0.74$ nm. The crystallization behavior of form II is not well understood. Pure form II, free from any conformational defects and the presence of any other phases, has been obtained in oriented samples having a low degree of stereoregularity.[2,15] It also has been recently found in oriented samples having a high degree of stereoregularity, upon releasing the tension.[8,14,19] Lotz et al. have shown that form II can be also obtained from form III.[19]

† The Dutch Polymer Institute.
‡ European Synchrotron Radiation Facility.
§ University of Akron.

10.1021/ma0109119 CCC: $20.00
Published on Web 09/29/2001

In isotropic powder samples, form II has been always obtained together with form I in polymers having a low degree of stereoregularity,[8,13,15] except by quench precipitation from solution. However, the precipitated powders when characterized by solid-state ^{13}C NMR show the presence of conformational disorder.[13,14,20] This disorder is attributed to the presence of trans-planar segments connecting **s**(2/1)2 helical portions of chains. The resulting crystal structure presents kink bands.[13,20] Until now pure form II has not been found in powder samples.

Finally, form III and IV are metastable phases of s-PP. Form III is obtained on cold drawing of the samples quenched from the melt into an ice bath.[9] Form IV is obtained by exposing oriented samples of form III to solvents (e.g., benzene, toluene).[10]

In this paper we will show the thermodynamic stability region in the pressure (p)−temperature (T) phase diagram, for the two forms of sPP containing **s**(2/1)2 helical chains, i.e., forms I and II. This has been explored in three different samples with different tacticity and equilibrium melting temperature obtained from three different sources (see Experimental Section). Furthermore, we will demonstrate that a pure form II, free from any conformational defects, can be obtained when the sample is crystallized at elevated pressures and temperatures from the isotropic melt. This is the first time since 1967, when it was found by Natta−Corradini[2] in oriented samples, that form II of sPP, completely free from conformational defects, has been crystallized in powder sample.

2. Experimental Section

Experimental studies have been performed on syndiotactic polypropylene obtained from three different sources, Phillips Petroleum (USA), FINA Research (Belgium), and Professor Kaminsky, University of Hamburg (Germany). These samples were synthesized especially for fundamental studies, in laboratory scale quantities. The sample from Prof. Kaminsky had the highest stereoregularity, fully syndiotactic pentads [rrrr = 98%], and the highest melting temperature (156 °C) at atmospheric pressure. The $p-T$ phase diagram for all three samples was explored. No differences in the crystallographic nature of the different phases in the $p-T$ phase diagram were observed. However, the exact values of melting point differ for different samples with varying tacticity.

For our experiment, we have used piston cylinder pressure cell with diamond windows, similar to that of Hikosaka and Seto.[21] The sample, 0.4 mm thick, was placed between the two diamonds surrounded by Teflon rings. Pressure was exerted to the sample by means of two pistons, the motion to the pistons being provided by well-regulated nitrogen gas. It is to be noted that no gas came in contact with the sample. The maximum pressure achieved in this design was 5 kbar. At the desired pressure, the temperature of the sample could be varied from room temperature to 300 °C at varying heating rates, from 1 to 10 °C/min. The diamonds in the cell allowed us to perform in-situ X-ray studies in transmission through the cell. The in-situ X-ray experiments were performed at the Materials Science beamline ID11, ESRF, using monochromatic X-rays of wavelength 0.784 Å to overcome absorption from the diamond windows. Data were collected on a Frelon CCD detector mounted on an image intensifier. Each diffraction pattern was recorded for 30 s. Spatial correction of the 2D X-ray patterns and integration, to give intensity against scattering angle, were made using the FIT2D program, kindly provided by Dr. Hammersely, ESRF.

The starting material used for the experiments was a sPP sample crystallized from melt at a cooling rate of 10 °C/min. The experiments performed explore two different regions of the $p-T$ phase diagram, region I and region II, following the different paths shown in Figure 1. The heating rate used was 2 °C/min unless otherwise stated. The temperatures quoted in this paper are those monitored by a thermocouple placed close to the sample position within the pressure cell.

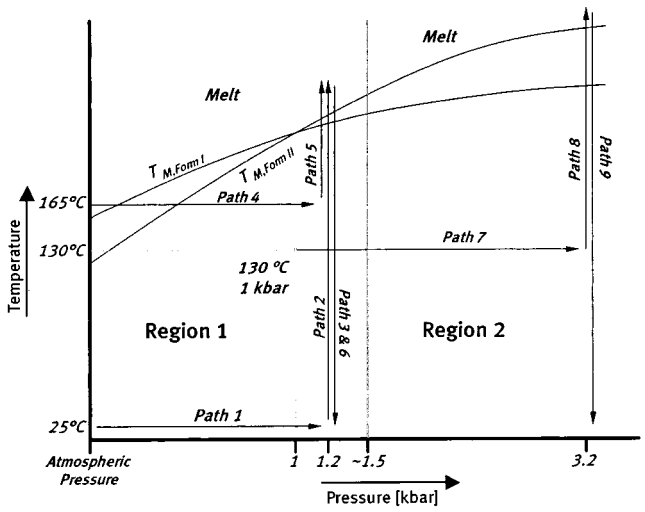

Figure 1. The figure above shows a series of paths in the pressure−temperature phase diagram along which the experiments have been performed. A demarcation line at approximately 1.5 kbar is drawn in the phase diagram. Experiments performed below 1.5 kbar, along paths 1−6, in region I of the phase diagram, show this region to be the thermodynamic stable region for form I. Whereas the experiments performed above 1.5 kbar, along paths 7, 8, and 9, in region II of the phase diagram, show this region to be the thermodynamic stable region for form II. The curved lines in the phase diagram show schematic variation in melting temperature of the two Forms at different pressures.

Solid-state ^{13}C nuclear magnetic resonance studies were performed on a Bruker spectrometer, on a sample crystallized by cooling the isotropic melt at 2 kbar, i.e., within the thermodynamically stable region for form II. To obtain a bigger sample for NMR studies, a different piston cylinder type pressure cell was used. WAXS pattern showed a sample rich in form II. However, small traces of form I were also present, probably because of the unavoidable temperature and pressure gradients present in thick samples within the pressure cell. Conditions for recording the solid-state NMR on the pressure-crystallized sample were similar to that mentioned in ref 13.

3. Results and Discussions

To explore the $p-T$ phase diagram, a series of experiments at different pressures and temperatures were performed. Experimental observations can be divided mainly into two different regions: region 1, below 1.5 kbar, where crystallization from the melt leads to the form I; and region 2, above 1.5 kbar where crystallization from the isotropic melt occurs directly in the form II. Since no differences in the crystalline structures were observed for samples with different tacticity, experimental observations made on the sample received from Professor Kaminsky, having stereoregularity of 98% [rrrr], are reported here.

3.1. Melting and Crystallization in Region I: Thermodynamically Stable Region for Form I_{per}. The starting sample of sPP was crystallized from the melt into form I_{imp}, at atmospheric pressure before being subjected to increasing pressure at room temperature. On increasing the pressure, the overall intensity of the diffraction pattern increased, indicating a total increase in crystallinity of the sample, but no phase transformation was observed. Crystallization may be enhanced due to greater supercooling at elevated pressures or forced

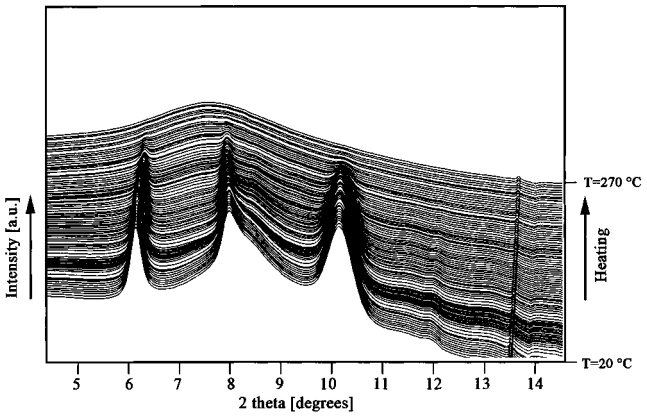

Figure 2. This figure shows a series of integrated WAXS patterns, of intensity against 2θ, recorded in situ while heating along path 2 in Figure 1. The starting material was crystallized from melt at atmospheric pressure in form I_{imp}. The heating rate was 2 °C/min. Each frame was recorded at a temperature interval of 2.5 °C. As evident from the last frame, the sample was molten at 270 °C. Wavelength used for the X-ray diffraction was 0.784 Å.

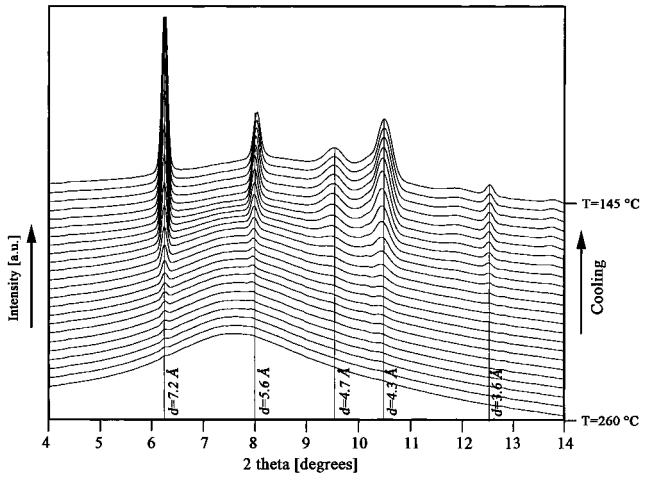

Figure 3. The figure here shows a series of X-ray diffraction patterns recorded while cooling from the melt along path 3 in the phase diagram, Figure 1. This series shows that crystallization from melt at these pressures occurs in form I_{per}. Cooling rate was 2 °C/min, and each frame was recorded at a temperature interval of 5 °C.

crystallization due to an overall increase in bulk density with the application of pressure. A small shift in the peak position of a few reflections occurs on increasing pressure.

After attaining the desired pressure of 1.2 kbar, along path 1 in Figure 1, the temperature was raised at a heating rate of 2 °C/min, along path 2. No changes in the form of crystallinity was observed during heating. The sample melted directly in form I_{imp} (Figure 2). Melting of form I_{imp} at these pressures seems similar to the usually observed melting behavior at atmospheric pressure. However, crystallization from the melt at these pressures is rather different from that anticipated at atmospheric pressure, as shown in Figure 3.

On cooling at a fixed pressure (1.2 kbar) at a rate of 2 °C/min, along path 3, the reflections at d = 7.2 Å (2θ = 6.2°), 5.6 Å (2θ = 8.0°), and 4.3 Å (2θ = 10.4°) appear and increase in intensity as the amorphous halo decreases (Figure 3). These reflections are common to all the known helical phases of sPP. On further cooling, at a supercooling of approximately 15 °C, a relatively

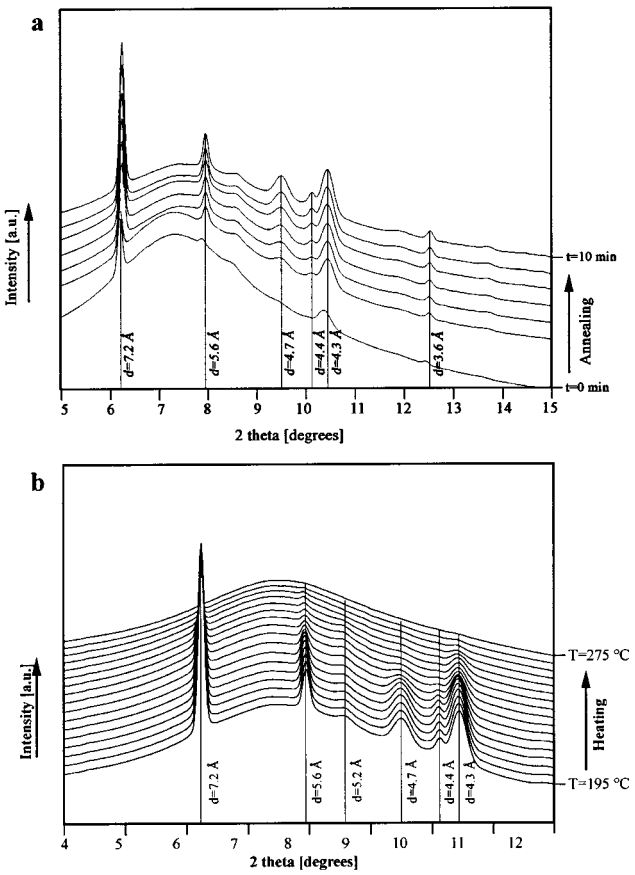

Figure 4. (a**)** This figure shows a series of X-ray diffraction patterns recorded while annealing the sample at a fixed pressure of 1.2 kbar and a temperature 165 °C. The sample was brought to the isobaric and isothermal condition on increasing the pressure of the melt along path 4. The melt had previously been obtained on heating the sample at atmospheric pressure. Each frame was recorded at a temperature interval of 100 s. (b**)** The annealed sample in (a) was heated along path 5 in the phase diagram (Figure 1). The X-ray diffraction patterns were recorded in situ while heating at the fixed pressure of 1.2 kbar. The heating rate was 2 °C/min. Each frame was recorded at a temperature interval of 5 °C.

broad reflection at d = 4.7 Å (2θ = 9.5°) and a rather weak reflection at 3.6 Å (2θ = 12.5°) can also be resolved. As described in ref 17, it is possible to evaluate the degree of order present in the structure of form I by measuring the ratio between the intensities of the (211) and (020) reflections at d = 4.7 and 5.6 Å, respectively. However, the intensity of the reflection at 4.7 Å, which is specific to form I_{per}, is relatively weak, and the peak is broad.[17] This suggests that crystallization into form I_{per} is not fully perfect when compared with the sample crystallized at high temperatures at atmospheric pressure. Earlier studies performed in isotropic sample, at atmospheric pressure, have shown the appearance of pure form I_{per} at very low supercoolings, when the sample was left to anneal for several weeks.[5,6,22]

To investigate the effect of annealing upon this form I, the following experiment was performed at isobaric and isothermal conditions, along path 4 as shown in Figure 1. The sample was melted at atmospheric pressure, and then the pressure was increased to 1.2 kbar, while holding at 165 °C. The melt was left to anneal under these conditions. Figure 4a shows a series of wide-angle X-ray diffraction patterns recorded during annealing. Initially, the same reflections as present in

Figure 3 were observed and increase in intensity with time. The reflection specific for form I_{per}, $d = 4.7$ Å ($2\theta = 9.5°$), appeared simultaneously with the other reflections, perhaps because of the relatively high supercooling. In addition, a further weak reflection at $d = 4.4$ Å ($2\theta = 10.2°$) appeared. These reflections are observed in form I_{per} for samples that were crystallized at high temperatures[17] at atmospheric pressure. The intensity of the reflections strengthen with increasing annealing time, suggesting an increase of the crystallinity and hence order in the crystals of form I_{per}. The appearance of the two reflections, at $d = 4.7$ and 4.4 Å, together with the other ($hk0$) reflections, strongly suggests that the crystals "perfected" upon annealing and are close to the ideal perfect form I[17] (compare Figure 3 with Figure 4a).

However, a rather weak reflection at $d = 5.2$ Å ($2\theta = 8.6°$) was also present with the other reflections. This reflection arises from the (110) plane in form II crystals. Since this peak is very weak in intensity, it is suggested that a few form II crystals were formed with the majority of material crystallizing in the more perfect state of the form I_{per}.

To compare the melting behavior of the "perfected" form I_{per} state to that shown earlier in Figure 2, the annealed sample, as in Figure 4a, was heated at a rate of 2 °C/min, at the same pressure of 1.2 kbar, along path 5 as shown in Figure 1. On heating, the intense reflections specific for the ordering of form I ($d = 4.7$ and 4.4 Å) decreased in intensity, while the weak 110 reflection of form II at 5.2 Å remained unchanged. This further strengthens the view that the origin of this reflection is due to the formation of crystals in form II. Furthermore, it suggests that form II crystals have a relatively higher melting temperature than the well-annealed form I crystals. These observations indicate that crystallization of the bulk of material in form I is kinetically more favorable compared to crystallization in form II, though the crystals of form II have a higher melting point.

Considering the reflections at 4.7 and 4.4 Å, which are indicative reflections for the ordering of form I, it could be concluded that for the same cooling rate crystallization in a more ordered form I from the melt is more favored at high pressures (<1.5 kbar) compared to crystallization at atmospheric pressure. Since the direct melting of form I_{imp} at a relatively low heating rate of 2 °C/min (Figure 2) occurred without the appearance of the reflections at $d = 4.7$ and 4.4 Å, annealing alone cannot overcome the imperfection within the crystals. Thus, it could be concluded that crystallization in form I_{per} is only feasible by melting the existing nuclei of form I_{imp} crystals. From these experimental observations it may be stated that if form I_{imp} is a defected state of form I_{per}, the origin of the defects exist primarily at the crystallographic level, which cannot be overcome without melting of the existing crystals (or nuclei).

3.2. Crystallization in Region II: Thermodynamically Stable Region for Form II. The appearance of form II on annealing and its high melting point, compared to that of form I_{per} at 1.2 kbar, suggests the existence of a thermodynamically stable region for form II in the proximity of the pressure region explored above. Experiments were performed, therefore, at higher pressures, i.e., within region II of the $p-T$ phase diagram (Figure 1).

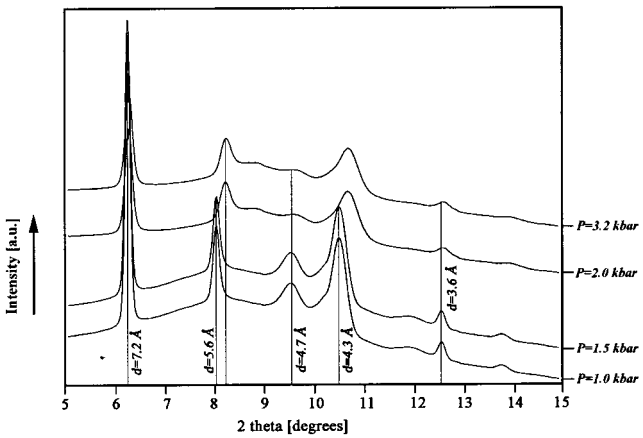

Figure 5. The sample crystallized along path 6 from the melt was brought to a pressure of 1 kbar and temperature 130 °C, before it was compressed to higher pressure (3.2 kbar) isothermally along path 7, shown in Figure 1. The figure above shows a series of X-ray diffraction patterns recorded in situ while increasing pressure isothermally along path 7. A shift in the peaks at 5.6 and 4.3 Å is noticed with increasing pressure from 1 to 3.2 kbar, whereas the position of the other peaks at 7.2 and 3.6 Å remains unchanged. The observed shift along the *b*-axis ($d = 5.6$ Å) results because of compression in the unit cell. The shift is discontinuous in nature and happens above 1.5 kbar.

In Figure 3 we showed that when a sample was cooled from the melt isobarically at 1.2 kbar, crystallization occurred directly in the more perfect state of form I, compared to crystallization upon cooling at the same rate at atmospheric pressure. A sample crystallized under conditions similar to that shown in Figure 3 was then subjected to pressure isothermally at 130 °C, from 1 to 3.2 kbar (along path 7, Figure 1) at a rate of 0.2 kbar/min. The intensity of all the reflections decreased and the reflections broadened and moved to lower d except for the (200) reflection ($d = 7.2$ Å). The reflection at $d = 5.6$ Å, assigned as (020) shifted to $d = 5.4$ Å, suddenly above 1.5 kbar. This suggests that with increasing pressure there is a compression of 0.4 Å along the *b*-axis while the *a*-axis remains unaltered. It would appear therefore that form I is very much influenced by increase in pressure, forming a disordered form I, as seen by the broadening of the reflections. A weak broad reflection at 5.2 Å at the higher pressures can be assigned to (110) reflection specific to form II. Moreover, the (211) reflection at $d = 4.7$ Å, indicating the amount of ordering in form I, also diminishes on compression along path 7. The near disappearance of the (211) reflection suggests that the order in the form I is strongly influenced by increasing pressure. All these observations suggest that the sample at the elevated pressures, as shown in Figure 5, has two crystal modifications—one which may be named as compressed and disordered form I and the other consists of a small amount of form II crystals.

In summary, as shown in Figure 5 and discussed above, discontinuous change along the *b*-axis of the perfect form I occurs on compression above 1.5 kbar. Considering the discontinuous nature of the crystallographic changes on compression, the new X-ray diffraction pattern at 3.2 kbar can be assigned as the compressed disordered state of the perfect form I.

After attaining the desired pressure of 3.2 kbar isothermally, the sample consisting of the disordered form I and form II crystals was heated at a rate of 2

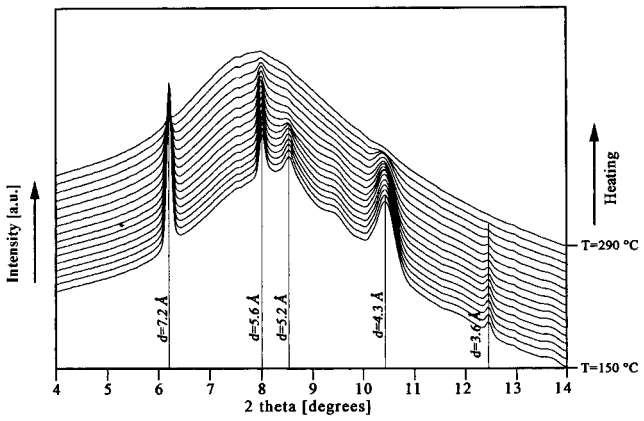

Figure 6. The figure above shows a series of X-ray diffraction patterns recorded in situ while increasing temperature at a fixed pressure of 3.2 kbar, along path 8. While the temperature is increased, the earlier shift observed in the reflections, on increasing pressure along path 7, reverts back. (For comparison, see X-ray diffraction pattern at 3.2 kbar in Figure 5.) The figure above shows the melting behavior of form I in region II of the phase diagram. Heating rate was 2 °C/min, and each frame was recorded at a temperature interval of 9 °C.

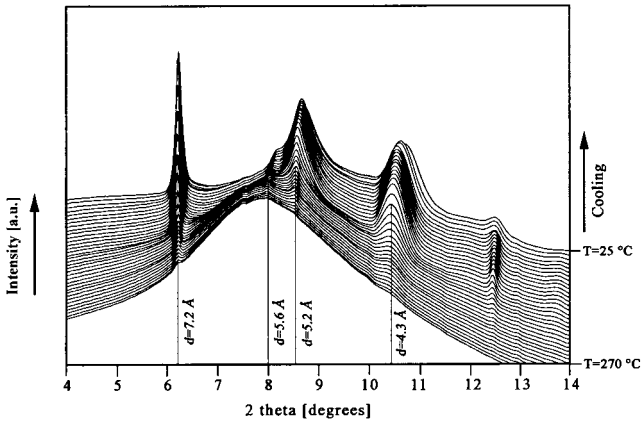

Figure 7. The figure shows a series of X-ray diffraction patterns recorded in situ while cooling the polymer at a fixed pressure of 3.2 kbar, along path 9 as shown in Figure 1. The comparison with Figure 3 shows that crystallization from melt, in region II of the $p-T$ phase diagram, occurs in form II. A weak reflection at 5.6 Å results from a few form I crystals present. Cooling rate was 2 °C/min, and each frame was recorded at a temperature interval of 7 °C.

°C/min. With increasing temperature, along path 8 in Figure 1, the shift of the (020) and other reflections, observed previously in Figure 5, reverted back; for comparison, see Figures 5 and 6. This suggests that the stresses developed during compression relax with heating of the sample. In addition, the reflection (110) of form II, at 5.2 Å, appeared to have sharpened and increased in intensity, suggesting that at these pressures form II is likely to be the thermodynamically stable phase. There is, however, a difference in the chiral arrangement of molecules in form II compared to form I, which means that form II cannot be formed without melting of the form I. To support this last statement, Figure 7 shows a series of X-ray diffraction patterns recorded during crystallization upon cooling, at a rate of 2 °C/min, from the isotropic melt at 3.2 kbar, along path 9 in Figure 1.

The appearance of weak reflections at $d = 7.2$, 5.6, and 4.3 Å occurred at a low supercooling of 10 °C. The position of these reflections suggests crystallization in form I, meaning that even at these high pressures crystallization in form I cannot be avoided at low supercoolings. However, on cooling further the reflection at $d = 5.2$ Å ($2\theta = 8.6°$) appeared. The intensity of this reflection, and those at 7.2 and 4.3 Å, increased with decreasing temperature, while the intensity of the reflection at $d = 5.6$ Å remained constant. These observations show that with decreasing temperature crystallization occurred directly in the form II, due to the appearance of the (110) reflection of form II at 5.2 Å, and at the end the bulk of the sample crystallized in form II, with a very small amount of form I present, which was formed at the very early stages of crystallization. When compared with Figures 3 and 4a, the obtained form I at 3.2 kbar shows more imperfection, because the reflections diagnostic to the form I_{per} are absent in Figure 7.

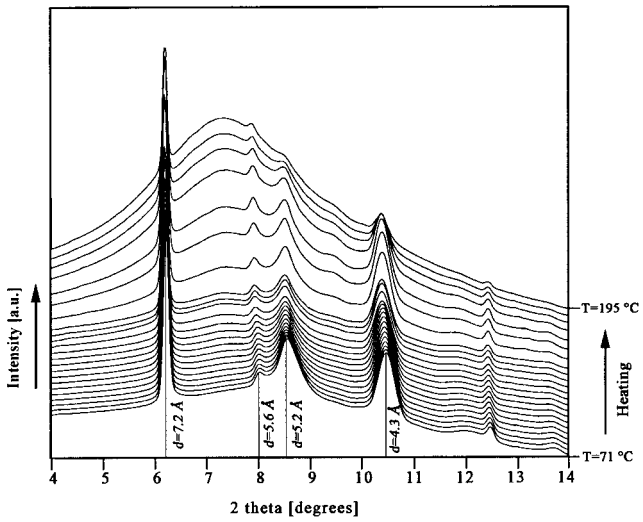

Figure 8. The figure shows melting of form II at atmospheric pressure. From a series of X-ray diffraction patterns recorded in situ, it is evident that on heating the strong reflections of form II disappear before the weak reflection at 5.6 Å; the latter corresponds to form I. Heating rate was 2 °C/min, and each frame was recorded at a temperature interval of 5.5 °C.

3.3. Melting of Form II Close to Atmospheric Pressure (200 bar). Above in Figures 2 and 4b, the melting behavior of form I was followed at atmospheric and elevated pressures. It was observed that at elevated pressure crystals in form II have a higher melting point than crystals in form I. To examine this effect further, a sample as crystallized at 3.2 kbar in Figure 7 was heated at 200 bar, close to atmospheric pressure. Figure 8 shows the melting behavior of this sample. Contrary to the melting behavior reported above in Figure 4b, the strong (110) reflection at 5.2 Å, specific to form II, disappeared whereas the weak (010) reflection, specific to form I, remained. These observations strongly suggest that at atmospheric pressure form I is the thermodynamically stable phase. On the other hand, at the elevated pressures, above 1.2 kbar, crystals in form I melted before those of form II, suggesting that at the higher pressures the form II is the thermodynamically stable phase.

3.4. Solid-State NMR Studies on Form II. From the experimental findings as reported above it has emerged conclusively that the thermodynamically stable region for form II exists above 1.5 kbar. Therefore, it has been possible to crystallize the sample directly from the isotropic melt into form II, at elevated pressures.

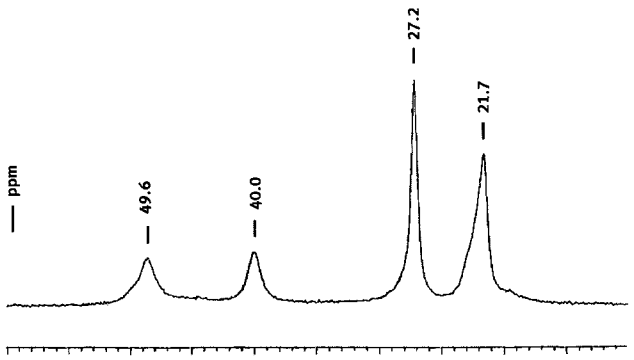

Figure 9. The figure shows solid-state ^{13}C NMR spectra recorded on the sample crystallized from the melt in region II of the $p-T$ phase diagram. The NMR spectrum shows the absence of defects in form II.

Previously, it has been shown that form II can be formed upon annealing the isotropic bulk at elevated temperatures for several days or weeks at atmospheric pressure[5,6] or by precipitation of sPP with methanol from a solution in *n*-pentane.[13] However, the samples thus crystallized always showed a conformational disorder as revealed by solid-state ^{13}C NMR.[13,14] Auriemma et al. by ^{13}C NMR[13,14] observed that the samples thus crystallized in form II consisted of more than four bands (located at 21.3, 26.7, 40.2, and 49.1 ppm) which can be assigned to pure **s**(2/1)2 helical conformation in the crystalline region of s-PP. In addition, three bands, two in the region of the methyl groups (18.9 and 22.4 ppm) and one in the region of the methylene group (44.9 ppm), were observed. Moreover, it was noted that the methyl group resonance with a maximum at 22.4 ppm contains a shoulder at about 23.4 ppm, and similarly the methine group shows a shoulder at approximately 17.6 ppm. The additional bands were associated with the presence of conformational disorder.

To examine the conformation of the sPP chains in form II, crystallized at elevated pressures and temperatures, we performed ^{13}C NMR studies (Figure 9). From this spectra, it is apparent that the chains are in the full TTGG helical conformation. The four bands, as observed, correspond to the anticipated crystalline component in s-PP. These bands can thus be assigned to the methyl signal (21.7 ppm), methine signal (27.2 ppm), and two methylene signals (40.0 and 49.6 ppm). The two methylene bands are separated by nearly 10 ppm. The one at 40.0 ppm originates from CH_2 in a GT.TG conformational environment (i.e., two γ gauche effects) and the second band at 49.6 ppm originates from CH_2 in a TG.GT conformational environment (i.e., zero γ gauche effects). The absence of the additional bands like in the case of Auriemma et al.[13,14] indicates that no conformational defects exist in the sample crystallized at the elevated pressures and temperatures in form II. In this respect, it is the first time that s-PP can be obtained as a polycrystalline unoriented material in the pure form II, i.e., Natta−Corradini phase,[2] free from any conformational defects. As reported above and in the literature, pure form II is usually obtained in oriented samples. In powder specimen, form II, when present, is full of defects frozen in the crystals, which are due to long portions of the chains in trans planar conformation, so forming kink bands.[13,14] Solid-state ^{13}C NMR allows a direct observation of such defects, since the methyl and methylene signals in the defect case, would present more peaks in the spectra.

4. Proposed Phase Diagram and Conclusions

From the experimental observations reported above on isotropic s-PP samples, the following conclusions can be drawn:

(a) On cooling from the melt at atmospheric pressure crystallization occurs in form I. On heating crystals of form I melt without any transformation (Figure 2). Thus, at atmospheric pressure form I should be the thermodynamically stable phase.

(b) When the sample is crystallized above 700 bar, crystallization mainly occurs in the more ordered state of form I, i.e., form I_{per}. On heating, crystals of form I melt directly without any transformation (Figures 2 and 4b). The sharpness of the (211) reflection at $d = 4.7$ Å (specific to form I) and the reflection at $d = 4.4$ Å (specific to form I_{per}) depends on the pressure at which crystallization is performed (for comparison see Figures 3 and 4a).

(c) Above 2 kbar, crystallization occurs in form II (Figure 7). At high pressures, crystals of form II melt directly at relatively higher temperatures compared to those of form I, suggesting high pressure to be the thermodynamically stable region for form II.

(d) Contrary to the melting behavior of form II above 2 kbar, the sample crystallized in form II (crystallized in the same conditions as in (c)) has a lower melting temperature than for form I, thus establishing the low-pressure region (<1.5 kbar) to be the thermodynamically stable region for form I. These findings strongly suggest that the crossover in the melting temperatures of the two different forms occurs below this pressure, i.e., at pressures <1.5 kbar, in the pressure−temperature phase diagram.

(e) NMR studies show that sample crystallized in form II on cooling the isotropic melt, above 2 kbar, is free of conformational defects.

From the above conclusions, a schematic pressure−temperature phase diagram showing the thermodynamic stability region for the two forms, I and II, can be drawn, as shown in Figure 1. From the phase diagram, it is evident that the chiral form II[2] has the thermodynamic stable regime above 1.5 kbar. Considering similar densities for the form II and form I, density cannot be considered as a reason for thermodynamic stability of the form II at elevated pressures and temperatures. However, a comparison of Figure 5 (last frame at 130 °C, 3.2 kbar) and Figure 7 (frames below and at 130 °C, 3.2 kbar) shows that at 3.2 kbar while the antichiral form I deforms on compression, the chiral form II remains unchanged. These findings suggest that though density of the two forms is similar, but when compared with the form I (having antichiral packing of the helices in the unit cell), the form II (having chiral packing of the helices within the unit cell) is more likely to withstand the compressive forces. In this respect, chains packed within the unit cell, having helical conformation and the same chirality, seem to be the thermodynamically favorable phase at extreme conditions like pressure. These observations may be of general relevance in the condensed matter physics, especially in the macromolecular physics where chirality plays a decisive role in crystallization.

Acknowledgment. The authors thank Prof. A. Grassi, University of Salerno, for performing the solid-state ^{13}C NMR measurements, and Dr. F. Auriemma and Prof. C. De Rosa of the University of Naples for

useful scientific discussions The authors extend their thanks to European Synchrotron Radiation Facility, Grenoble, for providing the experimental facilities. Further the authors thank Dr. J. Loos, Eindhoven University of Technology, for providing sPP samples from Prof. Kaminsky, University of Hamburg. The authors are grateful to Prof. B. Lotz, Strasbourg, for constructive discussions during the preparation of the manuscript. The authors dedicate this manuscript to Professor P. Corradini, University of Naples, for his 70th birthday, who proposed the form II in sPP dating back to 1967.

References and Notes

(1) Natta, G.; Corradini, P.; Ganis, P. *Makromol. Chem.* **1960**, *39*, 238.
(2) Corradini, P.; Natta, G.; Ganis, P.; Temussi, P. A. *J. Polym. Sci., Part C* **1967**, *16*, 2477.
(3) Natta, G.; Peraldo, M.; Allegra, G. *Makromol. Chem.* **1964**, *75*, 215.
(4) Lotz, B.; Lovinger, A. J.; Cais, R. E. *Macromolecules* **1988**, *21*, 2375.
(5) Lovinger, A. J.; Lotz, B.; Davis, D. D. *Polymer* **1990**, *31*, 2253.
(6) Lovinger, A. J.; Davis, D. D.; Lotz, B. *Macromolecules* **1991**, *24*, 552.
(7) Lovinger, A. J.; Lotz, B.; Davis, P. D.; Padden, F. J. *Macromolecules* **1993**, *26*, 3494.
(8) De Rosa, C.; Corradini, P. *Macromolecules* **1993**, *26*, 5711.
(9) Chatani, Y.; Maruyama, H.; Noguchi, K.; Asanuma, T.; Shiomura, T. *J. Polym. Sci., Part C* **1990**, *28*, 393.
(10) Chatani, Y.; Maruyama, H.; Asanuma, T.; Shiomura, T. *J. Polym. Sci., Part C* **1991**, *29*, 1649.
(11) Guadagno, L.; D'Aniello, C.; Naddeo, C.; Vittoria, V. *Macromolecules* **2000**, *33*, 6023.
(12) Auriemma, F.; De Rosa, C.; Corradini, P. *Macromolecules* **1993**, *26*, 5719.
(13) Auriemma, F.; Born, R.; Spiess, H.; De Rosa, C.; Corradini, P. *Macromolecules* **1995**, *28*, 6902.
(14) Auriemma, F.; Lewis, R. H.; Spiess, H. W.; De Rosa, C. *Macromol. Chem.* **1995**, *196*, 4011.
(15) De Rosa, C.; Auriemma, F.; Vinti, V. *Macromolecules* **1998**, *31*, 7430.
(16) Vittoria, V.; Guadagno, L.; Comotti, A.; Simonutti, R.; Auriemma, F.; De Rosa, C. *Macromolecules* **2000**, *33*, 6200.
(17) De Rosa, C.; Auriemma, F.; Vinti, V. *Macromolecules* **1997**, *30*, 4137.
(18) De Rosa, C.; Auriemma, F.; Corradini, P. *Macromolecules* **1996**, *29*, 7453.
(19) Lotz, B.; Mathieu, C.; Thierry, A.; Lovinger, A. J.; De Rosa, C.; Ruiz de Ballesteros, O.; Auriemma, F. *Macromolecules* **1998**, *31*, 9253.
(20) Auriemma, F.; De Rosa, C.; Ruiz de Ballesteros, O.; Corradini, P. *Macromolecules* **1997**, *30*, 6586.
(21) Hikosaka, M.; Seto, T. *Jpn. J. Appl. Phys.* **1982**, *21*, L332.
(22) Rodriguez-Arnold, J.; Bu, Z.; Cheng, S. Z. D. *J. Macromol. Sci., Rev. Macromol. Chem. Phys.* **1995**, *C35* (1), 117.

MA0109119